Solute Transport through Unsteady Hydrologic Systems Along a Plug Flow-to-Uniform Sampling Continuum

Stanley B. Grant[1,2], **Ciaran J. Harman**[3,4]

[1]Occoquan Watershed Monitoring Laboratory, The Charles E. Via, Jr. Department of Civil and Environmental Engineering, Virginia Tech, 9408 Prince William Street, Manassas VA 20110

[2]Center for Coastal Studies, Virginia Tech, 1068A Derring Hall (0420), Blacksburg, VA 24061

[3]Department of Environmental Health and Engineering, Johns Hopkins University, Baltimore, MD, USA

[4]Department of Earth and Planetary Science, Johns Hopkins University, Baltimore, MD, USA

Key Points:

- formulae are derived for age-ranked storage in, and solute transport through, unsteady hydrologic systems under shifted-uniform selection
- the SAS function's single parameter indicates where a system falls along a continuum between plug-flow and uniform sampling
- model predictions are concordant with published measurements of solute breakthrough in a sloping lysimeter subject to periodic wetting

Corresponding author: Stanley B. Grant, `stanleyg@vt.edu`

Abstract

Unsteady transit time distribution theory is a promising new approach for merging hydrologic and water quality models at the catchment scale. A major obstacle to widespread adoption of the theory, however, has been the specification of the StorAge Selection (SAS) function, which describes how the selection of water for outflow is biased by age. In this paper we hypothesize that some unsteady hydrologic systems of practical interest can be described, to first-order, by a "shifted-uniform" SAS that falls along a continuum between plug flow sampling (for which only the oldest water in storage is sampled for outflow) and uniform sampling (for which water in storage is sampled randomly for outflow). For this choice of SAS function, explicit formulae are derived for the evolving: (1) age distribution of water in storage; (2) age distribution of water in outflow; and (3) breakthrough concentration of a conservative solute under either continuous or impulsive addition. Model predictions conform closely to chloride and deuterium breakthrough curves measured previously in a sloping lysimeter subject to periodic wetting, although refinements of the model are needed to account for the reconfiguration of flow paths at high storage levels (the so-called inverse storage effect). The analytical results derived in this paper should lower the barrier to applying TTD theory in practice, ease the computational demands associated with simulating solute transport through complex hydrologic systems, and provide physical insights that might not be apparent from traditional numerical solutions of the governing equations.

Plain Language Summary

Many hydrologic systems, from hillslopes to water distribution systems, are intrinsically unsteady, by which we mean the flow of water and solutes varies continuously as a function of time. Historically, water quality models of such systems start by resolving the unsteady flow field first, and then "layering on" mass conservation laws in one-, two- or three-dimensions. A promising new approach, unsteady transit time distribution (TTD) theory, takes an entirely different tack, by tracking the flux and age distribution of water and solute moving into and out of a control volume drawn around the system of interest. Practical implementation of the theory requires choosing a storAge selection (SAS) function appropriate for the system under study. In this paper we propose a SAS function, which we call a "shifted-uniform SAS", that captures a continuum of physical behavior and thus may provide a first-order description of many natural and engineered

hydrologic systems. This choice of SAS function also leads to data-tested formulae for predicting water quality outcomes.

1 Introduction

Transit Time Distribution (TTD) theory elegantly addresses many long-standing challenges associated with modeling the age and transit times of water and solute in spatially heterogeneous hydrologic systems (McGuire and McDonnell (2006), McDonnell et al. (2010), Kirchner (2016)). Recently the theory has been extended to rigorously account for unsteady flow through the use of StorAge Selection, or SAS, functions (Botter et al. (2011), Rinaldo et al. (2015). A few definitions are in order. Here, "age" is the elapsed time a water parcel has spent in a hydrologic system, "transit time" is the age of a water parcel as it exits the system, and the SAS function approximates how water parcels exiting the system are biased by age. Because water parcels enter and exit a system at various times, all three quantities (i.e., age, transit time, and SAS function) are represented by probability distributions. Further, in unsteady hydrologic systems, the age and transit time distributions vary with time in accordance with an age conservation equation (ACE). The ACE, in turn, is a special case of the M'Kendrick-von Foerster (MKVF) equation (M'Kendrick (1925), von Foerster (1959)), which appears in many fields where age-dependent processes are important, including fluid mechanics, population dynamics, and chemical reactor design to name a few (Porporato and Calabrese (2015)).

Key strengths of unsteady TTD theory include its inclusion of both external forcing and internal variability (e.g., associated with the arrangement of flow pathways through a system, as well as the time-varying partitioning of water and solute along these flow pathways) (Porporato and Calabrese (2015), Kim et al. (2016)), conceptual simplicity, and potential for scale-up to natural and urban catchments (Rodriguez et al. (2018)). A significant challenge, at present, is the selection of the SAS function. This function, which gives the fraction of outflow drawn from each age-ranked volume-increment of water in storage, is an emergent property of the physics, biology and chemistry underlying water and solute transport through a particular system. In principal, the SAS function can be evaluated by volume averaging the advection-dispersion equation, although such an approach is practical only for the simplest of flow fields; e.g., one-dimensional, uniform and steady-state advection (Benettin et al. (2013)). In practice, one of several time-invariant probability distributions are often adopted, such as the uniform, Dirac

delta (for plug-flow), Beta, or Gamma distributions (Hrachowitz et al. (2016)). A major impediment to the broad application of unsteady TTD theory is the absence of a general framework for selecting the SAS function that best represents water and solute movement through a particular system, as well as the time-invariant nature of the standard distributions.

Here we propose and discuss a SAS functional form, which we call the "shifted-uniform SAS," that has the advantage of being: (1) parsimonious (it has one free parameter); (2) able to capture key emergent structural properties of certain hydrologic systems; (3) solvable analytically in terms of simple integrals of the time-varying fluxes and storage; (4) extensible to the case where the SAS itself varies with time (e.g., in response to changing storage levels (Kim et al. (2016)); and (5) a generalization of commonly-assumed steady-state transit time distributions. The shifted-uniform SAS selects water for outflow along a continuum from pure plug flow sampling (for which only the oldest water in storage is selected for outflow) to pure random or "uniform" sampling (for which all water in storage has an equal probability of being selected for outflow regardless of its age). These two end-members represent conceptual limits for solute transport by, respectively, advection (plug flow sampling) and dispersive spreading (uniform sampling). Because advection and dispersive spreading are universal controls on solute transport through environmental matrices, we hypothesize that many unsteady hydrologic systems can be situated along a continuum between these two limits. The closed-form solutions derived here, in particular, should lower the barrier to applying the framework in practice, yield physical insights not apparent from numerical solutions, and provide a mathematical foundation for linking hydrological and water quality models at the catchment scale (Hrachowitz et al. (2016)).

The paper is organized as follows. In Section 2 we present a step-by-step process for estimating the evolution of water age and solute breakthrough in a generic unsteady hydrologic system, and introduce the shifted-uniform SAS. This step-by-step process is then implemented for the shifted-uniform SAS in Section 3, leading to a set of closed form solutions for the age and transit time distributions, and for solute breakthrough under continuous and impulsive solute loading. In Section 4 the shifted-uniform model's single parameter is inferred from previously published measurements of conservative tracer transport through an experimental lysimeter subject to periodic wetting (Kim et al. (2016)). Discussion and conclusions are presented in Sections 5 and 6, respectively.

2 Step-by-step Application of the Unsteady TTD Framework

Our application of the unsteady TTD framework is implemented in four steps: (1) a dynamic water balance is performed over a control volume drawn around the system of interest; (2) a SAS function (i.e., a probability distribution and its parameters) is chosen; (3) the ACE is solved to yield the age distributions of water in storage and outflow; and (4) the solute concentration leaving the control volume is calculated by convolving the time history of solute concentration entering the system with the age distribution of water in outflow, after accounting for any age-dependent reactions. These steps are described next.

2.1 Performing a Dynamic Water Balance (Step 1)

The process begins by drawing a control volume around the hydrologic system of interest (Figure (1a)). A dynamic water balance over the control volume is then performed by measuring inflows and outflows (as was done in the experiments described later) or by solving physics-based models of flow through the system subject to some external forcing. Outputs from this step include the inflow of water to the control volume $J(t)$ [L T^{-1}], the outflow of water from the control volume $Q(t)$ [L T^{-1}], and the volume of water stored in the control volume $S(t)$ [L] as a function of time t (note that all flows and volumes are normalized by the surface area of the system). In the vadose zone, for example, rainfall may be the primary inflow while both discharge and evapotranspiration contribute to outflow. In an urban river, inflows might include industrial and wastewater discharges, and outflows might include withdrawals for agriculture and drinking water supply. For the sake of simplicity and without loss of generality, in what follows we will adopt a single inflow and outflow term ($J(t)$ and $Q(t)$, respectively).

2.2 Selecting a StorAge Selection (SAS) Function (Step 2)

From the dynamic water balance carried out in the last step, unsteady TTD framework aims to estimate the time varying age distribution of water in the control volume (i.e., the residence time distribution or RTD), and the age distribution of water exiting the control volume (i.e., the TTD). Conceptually, the TTD must be sampled from the RTD. The SAS function, $\Omega(S_T(T,t),t)$ [-], is a lumped approximation of this sampling

process:

$$P_{\mathrm{Q}}(T,t) = \Omega(S_T(T,t),t) \tag{1}$$

Here, $P_{\mathrm{Q}}(T,t)$ [-] is the cumulative distribution function (CDF) form of the TTD, while $S_T(T,t)$ [L] is the age-ranked storage function, defined as the volume of water in storage with ages less than or equal to T. Mathematically, the age-ranked storage function is the product of the volume of water in storage, $S(t)$, and the CDF form of the RTD, $P_{\mathrm{RTD}}(T,t)$ [-]: $S_T(T,t) = S(t) \times P_{\mathrm{RTD}}(T,t)$. Thus, the SAS function relates the transit time distribution of water leaving the control volume to the age distribution and volume of water stored in the control volume (equation (1)).

In this study we hypothesize that many hydrologic systems of practical interest can be described by a SAS that captures two key physical processes (Figure (1b)): (1) younger water travels some (storage-dependent) distance through the system before it can be sampled for discharge; and (2) older water in the system is sampled more-or-less randomly by age, reflecting the various flow paths water travels through the control volume before exiting. The shifted-uniform SAS function meets both requirements, where the fraction $p \in [0,1]$ is the percentile of the youngest age-ranked storage not sampled for discharge:

$$P_Q(T,t) = \Omega(S_T,t) = H(S_T(T,t) - pS(t))\frac{S_T(T,t) - pS(t)}{(1-p)S(t)} \tag{2}$$

The model's single parameter, p, must be inferred, for example from measured solute breakthrough data, as described Section 4.

2.3 Solving the Age Conservation Equation (ACE) (Step 3)

With the water balance and SAS function in hand, the evolving age structure of water in the control volume can be ascertained by solving the ACE:

$$\frac{\partial S_T}{\partial t} = J(t) - Q(t)P_Q(T,t) - \frac{\partial S_T}{\partial T} \tag{3a}$$

$$S_T(T=0,t) = 0 \tag{3b}$$

$$S_T(T,t=0) = S_0 H(T - T_0) \tag{3c}$$

$$H(x) = \begin{cases} 0, x < 0 \\ 1, x \geq 0 \end{cases} \tag{3d}$$

As written, the ACE equates the time rate of change of age-ranked storage (left hand side) to the inflow of water of age $T = 0$ (first term on right hand side); discharge

of water from the control volume with age distribution $P_Q(T,t)$ (second term); and aging of water in storage (third term). The boundary condition (equation (3b)) ensures that no water in storage has an age less than $T = 0$. The initial condition (equation (3c)) implies that all water in storage at time $t = 0$, $S(0) = S_0$, has a single age, $T = T_0$. In general, the age distribution of this *original* water is unknown (and likely unknowable), but by mathematically tagging it with an age of $T = T_0$ we can evaluate how quickly the initial condition's influence on age-ranked storage fades away with time (as demonstrated in Section 4). As noted earlier, the distributions, $P_{\mathrm{RTD}}(T,t)$ and $P_Q(T,t)$ are expressed as CDFs, and thus represent the fraction of water in storage (RTD) or exiting the control volume (TTD) with ages less than or equal to T at time t. The function $H(\cdot)$ is a unit step or Heaviside function.

After substituting the SAS function (from Step 2), equation (3a) can be solved either numerically or analytically to yield the age-ranked storage function, $S_T(T,t)$. The time-dependent RTD and TTD functions follow by substituting the solution for $S_T(T,t)$ into a rearranged version of the age-ranked storage definition, $P_{\mathrm{RTD}}(T,t) = \frac{S_T(T,t)}{S(t)}$, and equation (1), respectively.

2.4 Calculating Solute Breakthrough (Step 4)

From the foregoing results, the time-evolution of solute concentration in water exiting the control volume, $C_Q(t)$ [M L^{-3}], is calculated by convolving the probability density function (PDF) form of the TTD, $p_Q(T,t)$ [T^{-1}], with the time history of solute entering the control volume with inflow, $C_J(t)$ [M L^{-3}]:

$$C_Q(t) = \int_0^t C_J(t-T)p_Q(T,t)dT \tag{4a}$$

$$p_Q(T,t) = \frac{\partial P_Q}{\partial T} \tag{4b}$$

In the next section we derive and discuss a set of closed-form solutions for the age distribution, transit time distribution and solute breakthrough concentration under shifted-uniform sampling. These solutions are generic, in that they apply to any lumped system for which the time-dependence of inflows, outflows and storage is known (see Step 1 above).

3 Age and Solute Breakthrough under Shifted-Uniform Sampling

3.1 Representing the Shifted-Uniform SAS as Two Tanks in Series

The shifted-uniform SAS is mathematically equivalent to two tanks in series (Figure (1c)). Tank 1 has volume $S_1(t) = pS(t)$, intercepts all inflow, $J(t)$, of age $T = 0$ and solute concentration $C_J(t)$ across the control volume's upper boundary, and discharges to the next tank only its oldest water and solute under plug flow sampling where $H(\cdot)$ is a unit step or Heaviside function (equation (3d)):

$$\Omega_1(S_{T1}(T,t),t) = H(S_{T1}(T,t) - pS(t)) \tag{5}$$

Tank 2 has volume $S_2(t) = (1-p)S(t)$, receives only the oldest water and solute from Tank 1, and selects water and solute uniformly for discharge across the control volume's lower boundary:

$$\Omega_2(S_{T2},t) = \frac{S_{T2}(T,t)}{(1-p)S(t)} \tag{6}$$

The transfer of water volume between tanks, $Q_\Delta(t)$ [L T^{-1}], is prescribed so as to ensure that water balance over the control volume is maintained.

$$Q_\Delta(t) = (1-p)J(t) + pQ(t) \tag{7}$$

The system's overall age-ranked storage and RTD follow directly from the individual age-ranked storage functions for Tanks 1 and 2:

$$S_T(T,t) = S_{T1}(T,t) + S_{T2}(T,t) \tag{8a}$$

$$P_{\mathrm{RTD}}(T,t) = \frac{S_{T1}(T,t) + S_{T2}(T,t)}{S(t)} \tag{8b}$$

It is easy to demonstrate that a shifted-uniform SAS is mathematically equivalent to a series arrangement of plug flow and uniform SAS functions. The age distribution of water discharged from the control volume is the age distribution of water *discharged* from Tank 2 ($P_Q(T,t) = P_{Q2}(T,t)$) which, under uniform sampling, is equal to the age distribution of water *stored* in Tank 2. Therefore, from the definition of age-ranked storage (see equation (1) and discussion thereof), the age distribution of water discharged from the control volume is the ratio of the Tank 2 age-ranked storage and the water volume stored in Tank 2 at any time t: $P_Q(T,t) = P_{Q2}(T,t) = \frac{S_{T2}(T,t)}{(1-p)S(t)}$. Substituting this result into the SAS closure relationship, $\Omega(S_T(T,t),t) = P_Q(T,t)$, we obtain: $\Omega(S_T(T,t),t) = \frac{S_{T2}(T,t)}{(1-p)S(t)}$. Because all water in Tank 1 is younger than the youngest water in Tank 2, the age-ranked storage function for Tank 2 can be expressed as the difference between the

overall age-ranked storage function, $S_T(T,t)$, and the volume of water stored in Tank 1, $pS(t)$: $S_{T2}(T,t) = S_T(T,t) - pS(t)$ for $S_T(T,t) > pS(t)$. Combining these results, we arrive at equation (2), proving that our tank-in-series model is mathematically equivalent to a shifted-uniform SAS for the control volume.

The age structure of water in Tanks 1 and 2 can be determined by solving the ACE separately for each tank, provided that the age distribution of water flowing out of Tank 1 equals the age distribution of water flowing into Tank 2. Closed-form solutions for the age-ranked storage functions in Tanks 1 and 2 are presented next.

3.2 Age-Ranked Storage in Tank 1

Substituting the plug flow SAS (equation (5)) and transferring equations (3a), (3b) and (3c) into the Laplace domain, the following solution for age-ranked storage in Tank 1 can be derived (Text 1, supplemental information):

$$S_{T1}(T,t) = \begin{cases} pS_0 - \bar{Q}_\Delta(t) + \bar{J}(t), \ T = T_0 + t \\ \bar{J}(t), \ t \le T < T_0 + t \\ \bar{J}(t) - \bar{J}(t-T), \ 0 \le T < t \end{cases} \qquad 0 \le t \le t_c \tag{9a}$$

$$S_{T1}(T,t) = \bar{J}(t) - \bar{J}(t-T), \quad 0 \le T \le T_{m1}(t), \quad t > t_c \tag{9b}$$

The new functions $\bar{J}(t)$ [L], $\bar{Q}(t)$ [L] and $\bar{Q}_\Delta(t)$ [L] represent the cumulative area-normalized volume of water, as of time t, added to the control volume by inflow, exiting the control volume by outflow, and transferred between Tanks 1 and 2, respectively:

$$\bar{J}(t) = \int_0^t J(\nu)\, d\nu \tag{10a}$$

$$\bar{Q}(t) = \int_0^t Q(\nu)\, d\nu \tag{10b}$$

$$\bar{Q}_\Delta(t) = (1-p)\bar{J}(t) + p\bar{Q}(t) \tag{10c}$$

The solution for age-ranked storage in Tank 1 ($S_{T1}(T,t)$, equations (9a) and (9b)) takes on different functional forms depending on the choice of the age variable, T, and whether the elapsed time, t, is before or after a critical time, t_c [T]. The critical time is defined as the elapsed time at which all original water (i.e., water that was initially present in the control volume at time, $t = 0$) has been drained from Tank 1. It plays an important role in our solution by directly influencing the maximum age of water in Tank 1, which we denote by the variable $T_{m1}(t)$ [T]. In our two-tank representation of the con-

trol volume (Figure 1b), only the oldest water in Tank 1 (i.e., water with age $T_{m1}(t)$) is transferred from Tank 1 to Tank 2. Before the critical time, $t \leq t_c$, the oldest water in Tank 1 is original water. Because this original water is mathematically tagged with an age of T_0 at time $t = 0$ (see equation (3c) and discussion thereof), its age at any later time is: $T_{m1}(t \leq t_c) = T_0 + t$. After the critical time, $t > t_c$, an expression for the maximum age of water in Tank 1 can be derived by noting that, when the age variable is set equal to the maximum age of water in Tank 1, the age-ranked storage function must equal the total volume of water in Tank 1: $S_{T1}(T_{m1}(t), t) = S_1(t) = pS(t)$. Substituting equation (9b), we arrive at the following implicit solution for the maximum age of water in Tank 1 after the critical time:

$$pS(t) = \bar{J}(t) - \bar{J}(t - T_{m1}(t)),\ t > t_c \tag{11}$$

The critical time t_c, in turn, can be estimated directly from the control volume water balance, as the time required to drain all original water from Tank 1, where S_0 is the volume of original water in storage at time $t = 0$:

$$pS_0 = \bar{Q}_\Delta(t_c) \tag{12}$$

A graphical interpretation of this solution is presented in the supplemental information (Text 2).

3.3 Solution for Age-Ranked Storage in Tank 2

Substituting the uniform SAS (equation (6)), setting the age distribution and flow entering Tank 2 equal to the age distribution and flow leaving Tank 1, and transferring the ACE into the Laplace domain, we obtain the following solution for age-ranked storage in Tank 2 (Text 3, supplemental information):

$$S_{T2}(T,t) = \begin{cases} (1-p)S_0 e^{-\bar{\tau}(t)} + \int_0^t e^{-\bar{\tau}(t,\nu)} Q_\Delta(\nu)\, d\nu,\ T = T_0 + t \\ 0,\ \ 0 \leq T < T_0 + t \end{cases} \qquad 0 \leq t \leq t_c \tag{13a}$$

$$S_{T2}(T,t) = \begin{cases} (1-p)S_0 e^{-\bar{\tau}(t)} + \int_0^t e^{-\bar{\tau}(t,\nu)} Q_\Delta(\nu)\, d\nu,\ T = T_0 + t \\ \int_{t_c}^t e^{-\bar{\tau}(t,\nu)} Q_\Delta(\nu)\, d\nu,\ \ t \leq T < T_0 + t \\ \int_{t_{\mathrm{BT}}(t-T)}^t e^{-\bar{\tau}(t,\nu)} Q_\Delta(\nu)\, d\nu,\ \ T_{m1}(t) \leq T < t \\ 0,\ \ 0 \leq T < T_{m1}(t) \end{cases} \qquad t > t_c \tag{13b}$$

Here again the functional form of age-ranked storage depends on the magnitude of the age variable, T, and whether elapsed time is before ($t \leq t_c$) or after ($t > t_c$) the critical time (see equation (12) and discussion thereof). The new functions $\bar{\tau}(t)$ and $\bar{\tau}(t, \nu)$ [-] represent discharge-weighted time over the time intervals [0,t] and [ν,t], respectively.

$$\bar{\tau}(t) = \int_0^t \frac{Q(r)}{(1-p)S(r)}\, dr \tag{14a}$$

$$\bar{\tau}(t, \nu) = \bar{\tau}(t) - \bar{\tau}(\nu) \tag{14b}$$

The "breakthrough time" appearing in equation (13b), $t_{\mathrm{BT}}(t-T)$, represents the time at which a water parcel is transferred from Tank 1 to Tank 2, conditioned on the same water parcel entering Tank 1 at time $t_i = t-T$. An implicit expression for $t_{\mathrm{BT}}(t-T)$ can be derived by noting that, after the critical time t_c, a water parcel leaving Tank 1 at time t_{BT} must have entered Tank 1 at time, $t_i = t_{\mathrm{BT}} - T_{m1}(t_{\mathrm{BT}})$ (because Tank 1's plug flow SAS selects only the oldest water, of age T_{m1}, from storage for transfer to Tank 2). Likewise, a water parcel in Tank 2 of age T at time t must have entered Tank 1 at time, $t_i = t - T$. Equating these two Tank 1 entrance times yields the following implicit relationship for the breakthrough time, t_{BT}:

$$t_{\mathrm{BT}} - T_{m1}(t_{\mathrm{BT}}) = t - T = t_i,\ t > t_c,\ T_{m1}(t) \leq T < t \tag{15}$$

A more formal derivation of this implicit solution for t_{BT} is presented in the supplemental information (Text 3). According to equation (15), given a time series for the maximum age of water in Tank 1 ($T_{m1}(t)$, which depends on the control volume water balance and choice of the fraction p, see equation (11)), the breakthrough time t_{BT} is solely a function of the time at which a water parcel entered the control volume across its upper boundary, t_i. A graphical interpretation of the solution for age-ranked storage in Tank 2 (equations (13a) and (13b)) is presented in the supplemental information (Text 4).

3.4 Solute Breakthrough under Continuous Loading

The solute concentration in water exiting the control volume, $C_Q(t)$, can be calculated from the above results by convolving the solute concentration entering the control volume, $C_J(t)$, with the PDF form of the age distribution of water leaving the control volume (see equation (4a) and discussion thereof). Under shifted-uniform selection, the transit time distribution of water leaving the control volume can be written as fol-

lows (derivation in supplemental information, Text 5):

$$p_Q^{\text{new}}(T,t) = \frac{J(t-T)}{(1-p)S(t)} e^{-\bar{\tau}(t,\, t_{\text{BT}}(t-T))}, \;\; T_{m1}(t) \le T \le t, \;\; t > t_c \tag{16}$$

The superscript "new" indicates this is the TTD of new water exiting the control volume (as opposed to "original water" that was initially present in storage at time $t = 0$). Under shifted-uniform sampling, new water cannot be discharged from the control volume until after it first enters Tank 2, which is why equation (16) is only valid after the critical time, $t > t_c$. The lower bound on the age variable, $T_{m1}(t) \le T$ is imposed because all water younger than $T_{m1}(t)$ still resides in Tank 1. The upper bound on the age variable, $T \le t$, is imposed because all new water entered the control volume after time, $t = 0$, and thus cannot be older than the elapsed time t.

Combining equations (4a) and (16) yields the following solution for solute breakthrough:

$$C_Q(t) = \begin{cases} 0, \;\; 0 \le t \le t_c \\ \frac{1}{(1-p)S(t)} \int_0^{t-T_{m1}(t)} C_J(t_i) J(t_i) e^{-\bar{\tau}(t,\, t_{\text{BT}}(t_i))} dt_i, \;\; t > t_c \end{cases} \tag{17}$$

As noted earlier, the dummy integration variable, $t_i = t - T$, is the time a water parcel entered the control volume conditioned on it having age T at time t, and the breakthrough time, $t_{\text{BT}}(t_i)$, represents the time at which a solute molecule is transferred from Tank 1 to Tank 2 conditioned on it entering Tank 1 at time $t = t_i = t - T$ (see equation (15) and discussion thereof).

3.5 Solute Breakthrough under Impulsive Loading

The above solution simplifies when solute enters the control volume in a single pulse:

$$C_J(t_i) = \frac{M''}{J(t_{\text{pulse}})} \delta(t_i - t_{\text{pulse}}) \tag{18}$$

Here, the variable t_{pulse} [T] is the time at which the solute pulse entered the control volume, the function $\delta(\cdot)$ [T^{-1}] is the Dirac Delta function and the variables M'' [M L^{-3}] and $J(t_{\text{pulse}})$ [L T^{-1}]represent, respectively, the solute mass per unit area of the pulse and flow entering the control volume with the pulse at time, t_{pulse}. Combining equations (17) and (18) we arrive at a remarkably simple algebraic solution for the solute breakthrough concentration, where the discharge-weighted time, $\bar{\tau}(t, t_{\text{BT}})$, is given by equa-

tion (14b):

$$C_Q(t, M'', t_{\mathrm{BT}}) = \frac{M''}{(1-p)S(t)} \times \begin{cases} 0, \ 0 \leq t < t_{\mathrm{BT}} \\ e^{-\bar{\tau}(t, t_{\mathrm{BT}})}, \ \ t \geq t_{\mathrm{BT}} \end{cases} \tag{19}$$

The breakthrough time, t_{BT}, represents the time at which a solute pulse entering the control volume at time, $t = t_{pulse}$, is transferred from Tank 1 to Tank 2 under plug flow sampling. The implicit solution for t_{BT} takes the following form, where the maximum age of water in Tank 1, T_{m1}, is determined by water balance over the control volume and choice of the parameter p (see equation (11) and discussion thereof):

$$t_{\mathrm{BT}} - T_{m1}(t_{\mathrm{BT}}) = t_{\mathrm{pulse}} \tag{20}$$

In the event that the solute pulse enters the control volume at time $t_{\mathrm{pulse}} = 0$, the breakthrough time reduces to the critical time, $t_{\mathrm{BT}} = t_c$; i.e., the time at which all original water is first drained from Tank 1 (see equation (12) and discussion thereof).

Equation (19) predicts that, following the impulsive addition of a conservative solute to an unsteady hydrologic system at time $t = t_{\mathrm{pulse}}$, the breakthrough concentration is zero as the solute moves through Tank 1 under plug flow sampling ($t < t_{\mathrm{BT}}$). At $t = t_{\mathrm{BT}}$, the solute pulse is transferred undiluted from Tank 1 to Tank 2, and the breakthrough concentration, which under uniform sampling is equal to the average solute concentration in Tank 2, jumps from zero to $C(t = t_{\mathrm{BT}}) = \frac{M''}{(1-p)S(t_{\mathrm{BT}})}$. This initial breakthrough concentration represents the dilution of the solute mass, M'', into the volume of water present in Tank 2 at the breakthrough time, $S_2(t_{\mathrm{BT}}) = (1-p)S(t_{\mathrm{BT}})$. For times, $t > t_{\mathrm{BT}}$, the breakthrough concentration declines more-or-less monotonically with discharge-weighted time. The inclusion of the phrase "more-or-less" acknowledges that, if storage were to decline due to loss of water from the control volume (e.g., by evaporation), the breakthrough concentration could increase, all else being equal. The lone SAS parameter, p, influences solute breakthrough in three ways, by changing: (1) the volume of water in Tank 2 appearing in the denominator of equation (19), $S_2(t) = (1-p)S(t)$; (2) the evolution of discharge-weighted time, $\bar{\tau}(t, t_{\mathrm{BT}})$ (see equation (14a)); and (3) the time t_{BT} at which breakthrough begins, by changing the time evolution of the maximum age of water in Tank 1 (equation (11)).

3.6 Solute Breakthrough for N Impulsive Events

By linear superposition, a solution can also be written for N discrete solute pulses, where M_i'' and $t_{\text{pulse},i}$ are, respectively, the mass per unit area and input time for the i-th pulse:

$$C_Q(t) = \sum_{i=1}^{N} C_Q(t, M_i'', t_{\text{BT},i}) \tag{21a}$$

$$t_{\text{BT},i} - T_{m1}(t_{\text{BT},i}) = t_{\text{pulse},i} \tag{21b}$$

Because the time interval between solute pulses can be arbitrarily small, this discrete solution for solute breakthrough can be applied (in lieu of the continuous solution, equation (17)) to a continuously varying input of solute (see Section 4).

3.7 Solute Breakthrough under Pure Plug Flow or Uniform Selection

Explicit expressions can also be derived for solute breakthrough under pure plug flow and pure uniform sampling, corresponding to the limits $p \to 1$ and 0, respectively. As outlined in supplemental information (Text 6), the predicted solute breakthrough under pure plug flow sampling is as follows:

$$C_Q^{\text{PF}}(t) = \begin{cases} 0, \ 0 \le t \le t_c^{\text{PF}} \\ C_J(t - T_m^{\text{PF}}(t)), 0 \le T_m^{\text{PF}} < t, \ t > t_c^{\text{PF}} \end{cases} \tag{22a}$$

$$S_0 = \bar{Q}(t_c^{\text{PF}}) \tag{22b}$$

$$S(t) = \bar{J}(t) - \bar{J}(t - T_m^{\text{PF}}), \quad t > t_c^{\text{PF}}, \ 0 \le T_m^{\text{PF}} \le t \tag{22c}$$

The solute breakthrough concentration is zero for times, $t \le t_c^{\text{PF}}$, because only original water, which here is assumed to be solute-free, is discharged from the control volume prior to the critical time. After the critical time and under pure plug flow sampling, the breakthrough solute concentration at time t is simply the inflow solute concentration that entered the control volume earlier at time, $t - T_m^{\text{PF}}(t)$, where $T_m^{\text{PF}}(t)$ is the maximum age of water in the control volume at time t. The critical time at which all original water is drained from the control volume, t_c^{PF}, and the maximum age of water in storage after the critical time, $T_m^{\text{PF}}(t)$ are given implicitly by the control volume water balance (equations (22b) and (22c), respectively).

Equation (23a) is the solution for solute breakthrough under uniform sampling (supplemental information Text 7, see also Bertuzzo et al. (2013), Parker et al. (2021)) :

$$C_Q^{\mathrm{U}}(t) = \frac{1}{S(t)} \int_0^t C_J(t_i) J(t_i) e^{-\bar{\tau}^{\mathrm{U}}(t,t_i)}\, dt_i \tag{23a}$$

$$\bar{\tau}^{\mathrm{U}}(t,t_i) = \int_{t_i}^t \frac{Q(\nu)}{S(\nu)} d\,\nu \tag{23b}$$

4 Application to Solute Transport through a Lysimeter

4.1 Experimental System and Unsteady Water Balance

As a first test of the shifted-uniform SAS, we turned to a previously published laboratory study of transient solute transport through a small (1 m deep, 0.5 m wide, and 2.0 m long) unvegetated lysimeter inclined at 10 degrees and filled with 0.95 m^3 of basaltic sandy loam (saturated hydraulic conductivity $\approx 10^{-4}$ m s^{-1} (van den Heuvel et al., 2018)) and 0.05 m^3 of gravel at the downstream seepage face (Pangle et al. (2015), Kim et al. (2016)). The lysimeter was irrigated twice per day for 28 days to simulate periodic rainfall events, some of which were spiked with chloride or deuterium as conservative tracers (Kim et al. (2016)). The concentration of chloride and deuterium in water draining from the lysimeter (tracer breakthrough curve) was measured over time at a nominal sampling frequency of 1 h^{-1}. The original data can be found at Kim et al. (2021).

The model was applied in three steps. First, we set about closing water balance over the lysimeter. As described in Kim et al. (2016), irrigation, discharge and storage were separately measured at a nominal sampling frequency of 1 $min.^{-1}$. However, these data could not be used directly because of water balance issues arising from loss of water by evaporation (≈78 mm), a leak in the bottom of the lysimeter (≈62 mm), and errors in the discharge and irrigation rate measurements (≈143 mm) (Kim, M., personnel communication). To close volume balance over the lysimeter on a minute-by-minute basis, and on the premise that inflow (measured with a magnetic flow meter) might be the least accurate of the three measurements (being subject to evaporation and overspray of the irrigation water), we calculated inflow from measured storage (estimated from continuous measurements of the lysimeter's weight and fifteen frequency-domain reflectometry probes) and measured outflow (from a tipping bucket): $J(t) = Q(t) + \frac{dS}{dt}$. The outcome was a 28-day timeseries (sampling frequency 1 $min.^{-1}$) of lysimeter inflow, outflow and storage (Step 1 in Section 2.1).

Second, with the water balance in hand and knowledge of which irrigation pulses were spiked with either chloride or deuterium (at fixed concentrations of 6915 μ mol l^{-1} and 743.3 per mil, respectively), separate values for the fraction p were inferred from the chloride and deuterium breakthrough measurements by minimizing the root-mean-square-error (RMSE) between experimental data and breakthrough concentrations predicted by the continuous form of the shifted-uniform solution (equation (17)). Calculations were carried out in Mathematica v.12 (Wolfram Research, Inc.).

4.2 Testing the Integral Form of the Breakthrough Solution

The integral form of the shifted-uniform solution (equation (17)) closely tracks the breakthrough of both chloride and deuterium tracers over the 56 irrigation cycles monitored by Kim et al. (2016) (compare blue curve with orange and green circles, Figure 2). The inferred $p-$values (0.24 $\pm$0.05 and 0.23 $\pm$0.07, respectively) imply that, at any given, time roughly 24% of the youngest water is transiting through Tank 1, while 76% of the oldest water is uniformly sampled for discharge from Tank 2. Also shown in Figure 2 are model predictions for solute breakthrough in the limits of pure uniform and pure plug flow sampling (equations (23a) and (22a), respectively). In the uniform sampling limit (thin solid black curve in Figure 2) model predicted solute breakthrough occurs prematurely (relative to the measured solute breakthrough) consistent with the fact that, in this limit, any solute entering the system is immediately subject to random sampling for discharge. In the plug flow sampling limit (thin dashed black curve in Figure 2), on the other hand, the predicted breakthrough curves are delayed between 17 and 39 hours (relative to the measured solute breakthrough) and the peak breakthrough tracer concentration equals the inflow tracer concentration. These last two observations can be explained by noting that, under pure plug flow sampling, solutes experience no spreading or dilution as they are transported through the control volume.

4.3 Testing the Impulsive Form of the Breakthrough Solution

In Kim et al.'s experiments, each tracer pulse was added to the irrigation water over some finite period of time. For the purposes of testing the impulsive model we can assume the tracer mass associated with each pulse was released all at once at the mid-point of the pulse. Substituting these values for M_i'' into equation (21a) and setting $p = 0.24$, we find that the predicted breakthrough curves for the impulsive solution (thick black

dashed curves in Figure 2) closely track both the integral form of the breakthrough solution (blue curves) and the measured chloride and deuterium breakthrough measurements (orange and green circles). Compared to the integral solution, the impulsive solution occasionally predicts a higher solute concentration just as the solute is first breaking through, consistent with the impulsive model's underlying assumption that all of the tracer mass enters the control volume at a single point in time. Indeed, the degree of concordance between the integral and impulsive breakthrough curves is remarkable considering the relatively small volume (ca., 1 m^3) of the experimental lysimeter. Based on these results, the simple (algebraic) impulsive solution for solute breakthrough under shifted-uniform sampling (equation (21a)) will likely suffice for most applications.

4.4 Model Bias and the Inverse Storage Effect

An examination of the difference between predicted and measured breakthrough concentrations, or model residuals, reveals model bias at two timescales (Figure 3). Following the first two chloride and deuterium tracer pulses (time range 100 to 150 hours) breakthrough concentrations predicted by the shifted-uniform model consistently exceed measured values (i.e., the residuals are consistently positive). This long-period bias, which is also evident in Figure 2, could signal an underlying issue with the shifted-uniform SAS function or uncertainties associated with the overall volume balance. For our TTD analysis, we closed volume balance by calculating inflow from measured discharge and storage data (see Section 4.1), but in so doing may have introduced systematic biases in the volume balance that could account for these long-period positive residuals (e.g., by artificially concentrating solute discharged from the system).

A short period bias is also evident in Figure 3, that manifests as negative or positive residuals during periods of high storage. Negative residuals occur at high storage immediately following the application of either chloride or deuterium tracers, while positive residuals occur at high storage in the intervals between tracer applications. This pattern indicates that the shifted-uniform SAS tends to under-sample young water during periods of high storage. That is, during periods of high storage following the application of a tracer-tagged pulse the shifted-uniform solution tends to under-sample tracer-tagged water (negative residuals), while during periods of high storage following the application of a tracer-free pulse the shifted-uniform solution tends to under-sample tracer-free water (positive residuals).

In their original analysis of these data, Kim et al. noted a similar pattern, whereby "younger water is released in greater proportion under wetter conditions than drier." This so-called inverse storage effect (ISE) appears to be associated with storage-dependent changes in the arrangement of, and partitioning between, internal flow pathways; for example, when water previously trapped in the unsaturated zone is mobilized as the water table rises during an irrigation event. A similar phenomenon has been noted at a larger scale for hillslopes (Benettin et al., 2017), which have "a preference for discharging old water under low precipitation and storage conditions and a preference for discharging young water under high precipitation and storage conditions" (van der Velde et al. (2012)). Possible mechanisms include activation of overland flow, macropore flow, and the rise of the water table into relatively transmissive horizons at high storage (Harman (2019)). In the context of our modeling framework, the ISE might be addressed by relaxing the assumption that the fraction p is constant, and instead let it vary inversely with the volume of water present in storage, $S(t)$ (Jackson et al., 2016). Studies are presently underway to evaluate this approach. Even in its current form (with p constant), however, the shifted-uniform provides provides a very good first-order approximation of the solute breakthrough patterns (Figure 2) and cumulative mass of solute discharged over time (bottom panels, Figure 3a and 3b) measured during the set of lysimeter experiments evaluated here.

4.5 Time Evolution of Age-Ranked Storage

In addition to predicting solute transport through unsteady hydrologic systems (see last section), our solutions for age-ranked storage allow us to examine how the age structure of water in storage and outflow evolves over time (Figure 4). In these simulations we marked original water with an initial age of $T_0 = 10$ hours, and thus all original water (below the thick dashed curve in each panel) ages linearly with time, $T = 10\text{h}+t$. The upper thin black curve in Figure 4a represents the boundary between age-ranked water stored in Tank 1 (above the curve) and age-ranked water in Tank 2 (below the curve). Under plug flow sampling, only the oldest water in Tank 1 is selected for transfer to Tank 2. Consequently, original water in Tank 1 is progressively depleted until, at the critical time (t_c =12.6 hours), all original water has been transferred to Tank 2 and Tank 1 storage consists exclusively of new water (the critical time coincides with the cross-over of the upper solid curve and the thick dashed curve in Figure 4a). By contrast, under shifted-

uniform selection original water is never entirely removed from Tank 2 (age-ranked storage below the thick dashed curve, Figure 4a), although its proportion of Tank 2 storage declines over time. Because the total volume of water added to the lysimeter during each irrigation event is less than the average storage in Tank 1, a finite volume of water from the penultimate irrigation event is retained in Tank 1 during each irrigation cycle. This observation, together with the periodic irrigation schedule adopted for this experiment explains why, after the critical time, new water injected from Tank 1 into Tank 2 tends to be about 17 hours old (denoted by the orange color, Figure 4a). By the end of the 80 hour simulation, water discharged from the lysimeter is an approximately 1:3 mixture of original water with a single age of 90 hours and new water ranging in age from 20 to 70 hours (under shifted uniform sampling, the age distribution of water discharged is equal to the age distribution of water stored in Tank 2, which in Figure 4a corresponds to all age-ranked storage between the upper and lower solid black curves).

The predicted age distributions of water in the plug-flow and uniform SAS limits are presented in Figures 4b and 4c, respectively. Under plug flow sampling only the oldest water in storage is selected for discharge, with the result that all original water is removed from the lysimeter by around 58 hours (denoted by the crossover of the thick dashed and solid curves near the bottom of Figure 4b). Compared to the shifted-uniform case described above, age-ranked storage in the plug-flow limit is substantially enriched in young water (compare Figures 4a and 4b). In the uniform SAS limit, on the other hand, there is substantially more original water in storage at the end of the 80 hour simulation and the age distribution as a whole skews older (compare Figures 4a and 4c). This last result can be rationalized by noting that, in the uniform SAS limit, original water is removed from storage at a slower rate, all else being equal, because original water constitutes a smaller fraction of the total volume of water being uniformly sampled for discharge.

5 Discussion

5.1 Physical Interpretation of the Shifted-Uniform Solution

In this study we hypothesized that a shifted-uniform SAS might provide a first-order accurate assessment of mass transport through unsteady hydrologic systems. Application of the shifted-uniform solution to previously published measurements of solute transport through an experimental lysimeter (Kim et al. (2016)) supports this hypothesis with

the caveat that, in its present form (i.e., with p constant) the model does not capture second-order effects associated with the storage-dependent rearrangement of internal flow paths.

The relative success of the shifted-uniform solution begs the question: why does this simple model work so well? The answer probably lies in the model's representation of two universal solute mass transport processes: advection along the fastest flow paths through a system (as represented by plug flow sampling of water and solute in Tank 1) and dispersive spreading and dilution (as represented by uniform sampling of water and solute in Tank 2). An estimate for the plug flow velocity through Tank 1, $v_1(t)$ [L T^{-1}], can be obtained from the ratio of the tank's depth, $pS(t)$, and the maximum age of water in Tank 1, $T_{m1}(t)$. Likewise, an effective dispersion coefficient for Tank 2, $D_2(t)$ [L^2 T^{-1}], can be estimated by dividing the mean residence time in Tank 2, $\mu_2(t)$ [T], into the square of the tank's depth, $(1-p)S(t)$.

$$v_1(t) = \frac{pS(t)}{T_{m1}(t)} \tag{24a}$$

$$D_2(t) = \frac{(1-p)^2 S^2(t)}{\mu_2(t)} \tag{24b}$$

$$\mu_2(t) = \frac{S_0}{S(t)} t e^{-\bar{\tau}(t)} + \frac{1}{(1-p)S(t)} \int_0^t (t-u) Q_\Delta(u) e^{-\bar{\tau}(t,u)}\, du \tag{24c}$$

The expression adopted here for the mean residence time in Tank 2 (equation (24c)) is the mean age of water in Tank 2 assuming that: (1) water entering the tank has an age of $T = 0$h and (2) water initially present in the tank at time $t = 0$ has an age of $T_0 =$ 0h (compare with equation (7c) in Parker et al. (2021)).

Applied to the lysimeter data (Figure 5), we find that, after a start-up period of roughly 100 hours, the maximum age in Tank 1 (equation (11)) and the mean residence time in Tank 2 (equation (24c)) fluctuate around 15.9 ± 2.7 and 47.6 ± 2.3 hours, respectively. The plug flow velocity estimated from equation (24a) (6.1 ± 1.2 mm h^{-1}) closely approximates the average infiltration rate into the lysimeter (6.7 ± 9.6 mm h^{-1}), consistent with our hypothesis that plug flow sampling of water and solutes in Tank 1 represents advective transport. The dispersion coefficient inferred from equation (24b) (5.1 ± 0.53×10^{-7} m^2 s^{-1}) is roughly 370 times larger than the molecular diffusion coefficient for chloride in water at 25°C (2.03×10^{-9} m^2 s^{-1}) (Rumble (2022)). When the inferred dispersion coefficient is divided by the average discharge velocity from Tank 2 (6.31 ± 3.82 mm h^{-1}) the resulting dispersivity (0.29 ± 0.18 m) is within the range, although

at the high end, of values reported previously for sandy media over similar transport distances ($O(1\text{m})$) (Gelhar et al. (1992)), not accounting for source dispersion which is likely operating here as well (Kim et al. (2016)). Thus, uniform sampling from Tank 2 approximates solute spreading by mechanical and source dispersion. In summary, these back-of-the-envelope calculations support the notion that shifted-uniform's predictive power stems from its faithful representation of unsteady advection and dispersive mixing.

5.2 Generalization to Field-Scale Systems

How might the results presented above be scaled-up to model the evolution of water age and solute transport through urban or natural catchments? One promising approach divides the overall catchment into a set of linked conceptual components, for example based on landscape features and their corresponding hydrologic response units (HRU) (Hrachowitz et al. (2014); Hrachowitz et al. (2016)). Unsteady solute transport through any particular HRU could be estimated, in principle, from either the continuous (integral) or pulse (algebraic) solutions derived here (equations (17) and (21a), respectively). Because any continuous input signal can be expressed as a series of closely spaced pulses, these two solutions yield essentially equivalent breakthrough curves, as demonstrated earlier for the lysimeter experiments (see Section 4). Solute transport through the HRU would depend on its dynamic water balance (inflows, outflows and storage) along with its assigned p-value; i.e., where the HRU falls on the spectrum from pure plug flow to pure uniform sampling. The overall catchment response follows by dynamically routing water volume and solute mass through the HRU network. In this conceptualization, the shifted-uniform solution provides the mathematical foundation for linking hydrology and water quality at the catchment scale (Hrachowitz et al., 2016).

Individual HRUs can be further disaggregated into networks of shifted-uniform solutions, for example with the goal of representing solute transport along parallel fast (preferential) and slow (translatory) flow paths in vadose zone and riparian systems (Kung et al. (2000); Kung et al. (2005); Kung et al. (2006); Scaini et al. (2017); Benettin et al. (2019); Hester and Fox (2020); Rinderer et al. (2021)). Here preferential flow paths (characterized by faster breakthrough and reduced mixing) will have p-values closer to unity (reflecting a bias toward plug flow sampling), lower overall storage volumes $S(t)$, and reduced time to breakthrough (as reflected in a reduced maximum age of water in Tank 1, $T_{m1}(t)$). Conversely, translatory flow paths (characterized by slower breakthrough and

increased dispersive and diffusive mixing) will have p-values intermediate between zero and unity (reflecting a balance between delayed breakthrough in Tank 1 and enhanced mixing in Tank 2), higher storage volumes $S(t)$, and increased time to breakthrough (i.e., larger $T_{m1}(t)$). Indeed, the advective velocity and dispersive and diffusive mixing along a particular flow path can be precisely "tuned" by adjusting the water balance and p-value for the flow path, using the expressions derived earlier for solute breakthrough velocity and diffusivity under shifted-uniform sampling (equations (24a) and (24b), respectively). Allowing for parallel fast and slow paths would also be consistent with field studies showing that, at the hillslope scale, streamflow is often a mixture of both event and pre-event water during storms (Hornberger et al. (1991); McDonnell and Beven (2014); Jackson et al. (2016)).

5.3 Capturing Evapotranspiration and Age-Dependent Reactions

The exact solutions presented above for age-ranked storage and solute breakthrough can be amended to include evapotranspiration, conditioned on some theory for how water selected for ET is biased by age. For example, if plant roots preferentially sample the oldest water in storage (as might occur at the end of a wet season, see Figure 6b in Hrachowitz et al. (2016)) it may be appropriate to incorporate ET as an additional outflow mechanism from Tank 2 under plug flow selection (which removes only the oldest water in storage). Following the same solution procedure outlined above for Tank 1, this can be accomplished mathematically by setting the age distribution of water leaving by ET equal to, $P_{ET} = H(T - T_{m2}(t))$, where $T_{m2}(t)$ [T] is the maximum age of water in Tank 2 as a function of time. As with Tank 1, the maximum age in Tank 2 will be equal to the age of original water, $T_{m2}(t) = t + T_0$, up until a critical time for Tank 2, t_{c2} [T]. After the critical time, the maximum age in Tank 2 is determined from the following implicit expression, which follows from the fact that the age ranked storage in Tank 2, evaluated at $T = T_{m2}(t)$, must equal the total storage in Tank 2: $S_{T2}(T_{m2}(t), t) = (1 - p)S(t)$.

Likewise, our solution for solute breakthrough under shifted-uniform selection can be easily amended to capture age-dependent reactions, by letting the input concentration, $C_J(t_i = t - T, T)$, encode both the time at which the solute of interest entered the control volume (as reflected in the functional dependence on t_i), as well as how the non-conservative solute either increases or decreases with age as it transits through the

system of interest (as reflected in the functional dependence on T): $C_Q(t) = \int_0^t C_J(t_i = t - T, T) p_{Q2}^{\text{new}}(T, t) dT$ where $t > t_c$ (compare with equation (4a)).

5.4 Relation to Previous Theories of Water Age in Hydrology

Our study builds on an extensive and rapidly growing literature on the evolution of water age in unsteady hydrologic systems (c.f., Rigon et al. (2016); Ginn et al. (2009)). For example, the analysis presented in this paper is complementary to the work by Porporato and Calabrese (2015), who derived TTDs for various choices of time-invariant age selection functions, as well as for a stochastic version of the MKVF equation described earlier (Section 1). Calabrese and Porporato (2015) derived a closed form solution for the TTD under plug flow sampling, which is superficially similar to our solution for Tank 1; however, these authors prescribed the age of the oldest water sampled for outflow, for example as sinusoidally varying in time, while the age of the oldest water in our solution is determined from a dynamic water balance over the control volume (equations (22a)-(22c)). Calabrese and Porporato (2017) presented a general solution to the linear version of the MKVF equation, along with several solutions for specific non-linear (power-law) formulations of the MKVF's loss function (analogous to the SAS function in the ACE). While our shifted-uniform SAS is also non-linear, to our knowledge the closed-form solutions derived in this study have not been described previously.

The idea presented earlier of forming parallel networks of shifted-uniform SAS solutions to represent fast and slow flow paths through unsteady hydrologic systems (Section 5.2) is reminiscent of previous efforts to characterize the influence of reaction pathway architecture on the age and transit time of soil organic matter (Manzoni et al. (2009)). Here the term "age" has the same meaning in both contexts; namely, the elapsed time since a water molecule (in our case) or an organic molecule (Manzoni et al.'s case) entered the system. On the other hand, the term "transit time" takes on different meanings. For Manzini et al., it refers to the elapsed time from when an organic molecule entered the system and was subsequently transferred out of the system by reaction (i.e., respiration). In our case, transit time refers to the elapsed time from when water and solute entered the control volume with inflow and left the control volume as outflow. Additionally, Manzoni et al.'s analysis assumes that the age and transit time distributions of soil organic matter are time-invariant, whereas both distributions vary with time in our analysis.

6 Conclusions

Unsteady TTD theory provides a simple and powerful approach for understanding, and potentially predicting, the transport and transformation of solutes through complex and time-varying natural and engineered hydrologic systems. At its core, the framework assumes that water leaving a hydrologic system is composed of a collection of water parcels of different ages that all reached the system outlet at the same time, and were consequently combined to yield the observed solute concentration discharged from the system. In the context of TTD theory, the "combining process" is carried out by the SAS function, which stipulates how the sampling of water in storage for outflow is biased by age. As noted by Hrachowitz et al. (2016), the SAS function therefore integrates two universal transport mechanisms that control solute transport and transformation in environmental matrices: (1) where and when a solute enters the system, which determines along which flow path the solute transits through the system (source or geomorphic dispersion) and (2) local variation in flow velocities along any particular flow path (kinematic or mechanical dispersion). Put another way, the SAS function is an emergent property of the physics (and depending on context, chemistry and biology) governing solute transport through a particular system, although general rules for its selection in practice remain elusive.

In this paper we propose and test what we call a shifted-uniform SAS, as a possible generic first-order description of solute transport through unsteady hydrologic systems. This SAS function, which can be represented mathematically by two-tanks in series, captures the combined influence of geomorphic and kinematic dispersion by imposing a storage-dependent minimum transit time through the system (upstream tank under plug flow sampling) and then randomly sampling the water and solutes that pass through the first step for outflow (downstream tank under uniform sampling). The SAS function's single parameter, p, determines how water stored in the system at any given time is partitioned between the upstream and downstream tanks, and thus where a particular hydrologic system falls along the plug-flow ($p \rightarrow 1$) to uniform ($p \rightarrow 0$) sampling continuum. In addition to providing a compelling conceptual framework, the two tank representation of the shifted-uniform SAS also opens the door to the derivation of explicit formulae for the age-structure of water in storage (equations (9a), (9b), (13a), and (13b)) and outflow (equation (16)), and for the solute breakthrough concentration under both continuous (equation (17)) and impulsive (equation (21a)) solute loading to the system.

Fitting equation (17) to previously published breakthrough measurements of chloride and deuterium in a sloping lysimeter subject to periodic wetting, we obtain an optimized value of about $p = 0.24$. The implied range of advective velocities and dispersivities (in Tanks 1 and 2, respectively) are very close to what we would expect for this experimental system (see Figure 5 and discussion thereof). It is important to stress that, although the shifted-uniform SAS is time-invariant, the residence time distribution of water in storage and the age distribution of water in outflow are both strongly time varying, as is evident from the predicted age-ranked storage in Tanks 1 and 2 over the first 80 hours of the lysimeter's operation (Figure 4a). Indeed, a weakness of the shifted-uniform SAS in its current form is precisely its time-invariance, specifically its inability to account for the enrichment of young water in outflow during periods of high storage. Allowing the fraction p to vary inversely with storage might address this so-called inverse storage effect, and efforts are currently underway to explore this possibility.

Acknowledgments

The authors declare no conflict of interest. SBG was supported by a U.S. National Science Foundation Growing Convergence Research Program award (NSF Award 2021015) and Virginia Tech's Charles E. Via, Jr. Department of Civil and Environmental Engineering; CH was supported by a U.S. National Science Foundation grant (NSF Award EAR-1654194). SBG and CH developed the modeling framework, SBG drafted the manuscript, both co-authors contributed edits. The lysimeter data is available in Hydroshare; see Kim et al. (2021). The authors thank the Associate Editor (Madan Jha) and the three reviewers (Amilcare Porporato and two anonymous) for their many helpful suggestions for improving the manuscript.

References

Benettin, P., Queloz, P., Benisomon, M., McDonnell, J., & Rinaldo, A. (2019). Velocities, residence times, tracer breakthroughs in a vegetated lysimeter: A multitracer experiment. *Water Resources Research*, *55*, 21-33. doi: https://doi.org/10.1002/2018WR023894

Benettin, P., Rinaldo, A., & Botter, G. (2013). Kinematics of age mixing in advection-dispersion models. *Water Resources Research*, *49*, 8539-8551. doi: https://dx.doi.org/10.1002/2013WR014708

Benettin, P., Soulsby, C., Birkel, C., Tetzlaff, D., Botter, G., & Rinaldo, A. (2017). Using SAS functions and high-resolution isotope data to unravel travel time distributions in headwater catchments. *Water Resources Research*, *53*, 1864-1878. doi: https://dx.doi.org/10.1002/2016WR020117

Bertuzzo, E., Thomet, M., Botter, G., & Rinaldo, A. (2013). Catchment-scale herbicides transport: Theory and application. *Advances in Water Resources*, *52*, 232-242. doi: https://dx.doi.org/10.1016/j.advwatres.2012.11.007

Botter, G., Beertuzzo, E., & Rinaldo, A. (2011). Catchment residence and travel time distributions: The master equation. *Geophysical Research Letters*, *38*, L11403. doi: https://dx.doi.org/10.1029/2011GL047666

Calabrese, S., & Porporato, A. (2015). Linking age, survival and transit time distributions. *Water Resources Research*, *51*, 8316-8330. doi: https://dx.doi.org/10.1002/2015WR017785

Calabrese, S., & Porporato, A. (2017). Multiple outflows, spatial components, and nonlinearities in age theory. *Water Resources Research*, *53*, 110-126. doi: https://dx.doi.org/10.1002/2016WR019227

Gelhar, L., Welty, C., & Rehfeldt, K. (1992). A critical review of data on field-scale dispersion in aquifers. *Water Resources Research*, *28*, 1955-1974. doi: https://doi.org/10.1029/92WR00607

Ginn, T., Haeri, H., Massoudieh, A., & Foglia, L. (2009). Notes on groundwater age in forward and inverse modeling. *Transport in Porous Media*, *79*, 117-134. doi: https://dx.doi.org/10.1007/s11242-009-9406

Harman, C. J. (2019). Age-ranked storage-discharge relations: A unified description of spatially lumped flow and water age in hydrologic systems. *Water Resources Research*, *55*, 7143-7165. doi: https://dx.doi.org/10.1029/2017WR022304

Hester, E., & Fox, G. (2020). Preferential flow in riparian groundwater: Gateways for watershed solute transport and implications for water quality management. *Water Resources Research*, *56*, e2020WR028186. doi: https://dx.doi.org/10.1029/2020WR028186

Hornberger, G., Germann, P., & Beven, K. (1991). Throughflow and solute transport in an isolated sloping soil block in a forested catchment. *Journal of Hydrology*, *124*, 81-89.

Hrachowitz, M., Benettin, P., van Brekelen, B. M., Fovet, O., Howden, J., Nicholas,

Ruiz, L., ... Wade, A. J. (2016). Transit times-the link between hydrology and water quality at the catchment scale. *WIREs Water*, *3*, 629-657. doi: https://dx.doi.org/10.1002/wat2.1155

Hrachowitz, M., Fovet, O., Ruiz, L., Euser, T., Gharari, S., Nijzink, R., ... Gascuel-Odoux, C. (2014). Process consistency in models: The importance of system signatures, expert knowledge, and process complexity. *Water Resources Research*, *50*, 7445-7469. doi: https://dx.doi.org/10.1002/2014WR015484

Jackson, C., Du, E., Klaus, J., Griffiths, N., Bitew, M., & McDonnell, J. (2016). Interactions among hydraulic conductivity distributions, subsurface topography, and transport thresholds revealed by a mutitracer hillslope irrigation experiment. *Water Resources Research*, *52*, 6186-6206. doi: https://dx.doi.org/10.1002/2015WR018364

Kim, M., Pangle, L. A., Cardoso, C., Lora, M., Volkmann, T. H., Wang, Y., ... Trock, P. A. (2016). Transit time distributions and storage selection functions in a sloping soil lysimeter with time-varying flow paths: Direct observation of internal and external transport variability. *Water Resources Research*, *52*, 7105-7129. doi: https://dx.doi.org/10.1002/2016WR018620

Kim, M., Volkmann, T. H. M., Wang, Y., Meira Neto, A. N., Katarena, M., Harman, C. J., & Troch, P. A. (2021). Biosphere 2 Landscape Evolution Observatory 2016 PERTH experiment - Dataset for the LEO east and west hillslopes. *HydroShare*. doi: 10.4211/hs.a74168d3396c436a8f0cd5910358df13

Kirchner, J. W. (2016). Aggregation in environmental systems–part 1: Seasonal tracer cycles quantify young water fractions, but not mean transit times, in spatially heterogeneous catchments. *Hydrology and Earth Systems Science*, *20*, 279-297. doi: https://doi.org/10.5194/hess-20-279-2016

Kung, K., Hanke, M., Helling, C., Kladivko, E., Gish, T., Steenhuis, T., & Jaynes, D. (2005). Quantifying pore-size spectrum of macropore-type preferential pathways. *Soil Science Society of America Journal*, *69*, 1196-1208. doi: https://dx.doi.org/10.2136/sssaj2004.0208

Kung, K., Kladivko, E., Gish, T., Steenhuis, T., Bubenzer, G., & Helling, C. (2000). Quantifying preferential flow by breakthrough of sequentially applied tracers: Silt loam soil. *Soil Science Society of America Journal*, *64*, 1296-1304. doi: https://dx.doi.org/10.2136/sssaj2000.6441296x

Kung, K., Kladivko, E., Helling, C., Gish, T., Steenhuis, T., & Jaynes, D. (2006). Quantifying pore-size spectrum of macropore-type preferential pathways under transient flow. *Vadose Zone Journal*, *5*, 978-989. doi: https://dx.doi.org/10.2136/vzj2006.0003

Manzoni, S., Katul, G., & Porporato, A. (2009). Analysis of soil carbon transit times and age distributions using network theories. *Journal of Geophysical Research: Biogeosciences*, *114*, G04025. doi: https://dx.doi.org/10.1029/2009JG001070

McDonnell, J., & Beven, K. (2014). Debates on water resources: The future of hydrological sciences: A (common) path forward? a call to action aimed at understanding velocities, celerities and residence time distributions of the headwater hydrograph. *Water Resources Research*, *50*, 5342-5350. doi: https://doi.org/10.1002/2013WR015141

McDonnell, J., McGuire, K., Aggarwal, P., Beven, K., Biondi, D., Destouni, G., ... Wrede, S. (2010). How old is streamwater? open questions in catchment transit time conceptualization, modelling and analysis. *Hydrological Processes*, *24*, 1745-1754. doi: https://dx.doi.org/10.1002/hyp.7796

McGuire, K., & McDonnell, J. (2006). A review and evaluation of catchment transit time modeling. *Journal of Hydrology*, *330*, 543-563. doi: https://doi.org/10.1016/j.jhydrol.2006.04.020

M'Kendrick, A. (1925). Applications of mathematics to medical problems. *Proc. Edinburgh Math. Soc.*, *44*, 98-130. doi: https://dx.doi.org/10.1002/2015WR017027

Pangle, L., S.B., D., ..., & Zeng, X. (2015). The landscape evolution observatory: A large-scale controllable infrastructure to study coupled earth-surface processes. *Geomorphology*, *244*, 190-203. doi: https://dx.doi.org/10.1016/j.geomorph.2015.01.020

Parker, E., Grant, S., Cao, Y., Rippy, M., McGuire, K., Holden, P., & et. al. (2021). Predicting solute transport through green storm water infrastructure with unsteady transit time distribution theory. *Water Resources Research*, *57*, e2020WR028579. doi: https://dx.doi.org/10.1029/2020WR028579

Porporato, A., & Calabrese, S. (2015). On the probabilistic structure of water age. *Water Resources Research*, *51*, 3588-3600. doi: https://dx.doi.org/10.1002/

2015WR017027

Rigon, R., Bancheri, M., & Green, T. (2016). Age-ranked hydrological budgets and a travel time description of catchment hydrology. *Hydrology and Earth System Sciences*, *20*, 4929-4947. doi: https://dx.doi.org/10.5194/hess-20-4929-2016

Rinaldo, A., Benettin, P., Harman, C. J., Hrachowitz, M., McGuire, K. J., van der Velde, Y., ... Botter, G. (2015). Storage selection functions: A coherent framework for quantifying how catchments store and release water and solutes. *Water Resources Research*, *51*, 4840-4847. doi: https://dx.doi.org/10.1002/2015WR017273

Rinderer, M., Krüger, J., Lang, F., Puhlmann, H., & Weiler, M. (2021). Subsurface flow and phosphorous dynamics in beech forest hillslopes during sprinkling experiments: how fast is phosphorous replenished? *Biogeosciences*, *18*, 1009-1027. doi: https://dx.doi.org/10.5194/bg-18-1009-2021

Rodriguez, N. B., McGuire, K. J., & Klaus, J. (2018). Time-varying storage-water age relationships in a catchment with a mediterranean climate. *Water Resources Research*, *54*, 3988-4008. doi: https://dx.doi.org/10.1029/2017WR021964

Rumble, J. (Ed.). (2022). *Handbook of chemistry and physics, 102nd edition.* Boca Raton, Florida, U.S.A.: CRC Press.

Scaini, A., Audebert, M., Hissler, C., Fenicia, F., Gourdol, L., Pfister, L., & Beven, K. (2017). Velocity and celerity dynamics at plot scale inferred from artificial tracing experiments and time-lapse ert. *Journal Hydrology*, *546*, 28-43. doi: https://dx.doi.org/10.1016/j.jhydrol.2016.12.035

van den Heuvel, D., Troch, P., Booij, M., Niu, G., Volkmann, T., & Pangle, L. (2018). Effects of differential hillslope-scale water retention characteristics on rainfall-runoff response at the landscape evolution observatory. *Hydrological Processes*, *32*, 2118-2127. doi: https://dx.doi.org/10.1002/hyp.13148

van der Velde, Y., Torfs, P., van der Zee, S., & Uijlenhoet, R. (2012). Quantifying catchment-scale mixing and its effect on time-varying travel time distributions. *Water Resources Research*, *48*, W06536. doi: https://doi.org/10.1002/2011WR011310

von Foerster, H. (1959). The kinetics of cellular proliferation. In J. Stohlman (Ed.), (p. 382-407). Grune and Stratton, N.Y.

7 Figure Legends

Figure 1: The Unsteady TTD framework described in this study aims to predict the evolution of water age and solute breakthrough in unsteady hydrologic systems. (a) The analysis begins by performing a water balance over a control volume drawn around the system of interest. In general, all water balance terms ($J(t)$, $Q(t)$, and $S(t)$) and solute concentrations ($C_J(t)$ and $C_Q(t)$) vary with time. The age of water entering the system is assumed to be $T = 0$, while the age distribution of water in storage ($P_{\mathrm{RTD}}(T,t)$) and outflow ($P_Q(T,t)$) both vary with time. (b) In this study we hypothesize that many hydrologic systems can be approximated by a shifted uniform SAS, $\Omega(S_T(t),t)$, in which the pth youngest fraction of water in storage is not sampled for outflow, while the $(1-p)$th oldest fraction is sampled uniformly for outflow. The SAS is represented here as a CDF. (c) The shifted-uniform SAS is mathematically equivalent to placing two tanks in series with volumes $S_1(t) = pS(t)$ and $S_2(t) = (1-p)S(t)$, respectively. Water leaves the first tank by plug flow sampling ($\Omega_1(S_{T1}(t),t)$), while water leaves the second tank by uniform sampling ($\Omega_2(S_{T2}(t),t)$). Flow of water volume between tanks is represented by the variable $Q_\Delta(t)$. The CDFs $P_{\mathrm{RTD1}}(T,t)$ and $P_{\mathrm{RTD2}}(T,t)$ are the age distributions of water in the first and second tanks.

Figure 2: Comparison of measured and predicted breakthrough of either (a) chloride or (b) deuterium tracer in an experimental lysimeter (bottom plots in each panel) subject to periodic irrigation (top plots in each panel) (data from Kim et al. (2016)). Predicted breakthrough concentrations are shown for plug flow sampling (thin dashed black curves), uniform sampling (thin solid black curves) and shifted uniform sampling with either the continuous solution (thick solid blue curve curves) or impulsive solution (thick dashed black curve). The inferred p values were 0.24 $\pm$0.05 and 0.23 $\pm$0.07 for, respectively, the chloride and deuterium breakthrough curves. Initial tracer concentrations were either 6915 μ mol l^{-1} or 743.3 per mil for chloride and deuterium, respectively. Model esiduals are plotted in Figure 3, while predictions for the maximum of age water in Tank 1 and the average age of water in Tank 2 are plotted in Figure 4.

Figure 3: A comparison of (a) chloride and (b) deuterium model residuals (upper panel) and the cumulative mass entering and exiting the lysimeter (lower panel). Residuals and predicted cumulative mass results were generated from the optimized shifted-uniform solution (blue curves in Figure 2).

Figure 4: Age-ranked storage during the first 80 hours of the lysimeter experiment calculated from equations (9a), (9b), (13a), and (13b) assuming: (a) shifted-uniform selection ($p = 0.24$); (b) pure plug-flow selection ($p = 1$); and (c) pure uniform selection $p = 0$. The heavy black dashed curve in each panel denotes the boundary between new water (above the curve) and original water (below the curve). The lower black solid curve in each panel indicates total storage at any particular time. In panel (a), the upper solid black curve denotes the boundary between water stored in Tank 1 (above the curve) and Tank 2 (below the curve). For these simulations we marked original water with an initial age of $T_0 = 10$ hours.

Figure 5: A physical interpretation of the shifted-uniform solution as applied to tracer transport through an experimental lysimeter, including inflow timeseries (top graph), maximum age and mean residence time of water in Tanks 1 and 2 (second graph), implied plug flow velocity through Tank 1 (third graph) and implied dispersion coefficient in Tank 2 (fourth graph).

Figure 1.

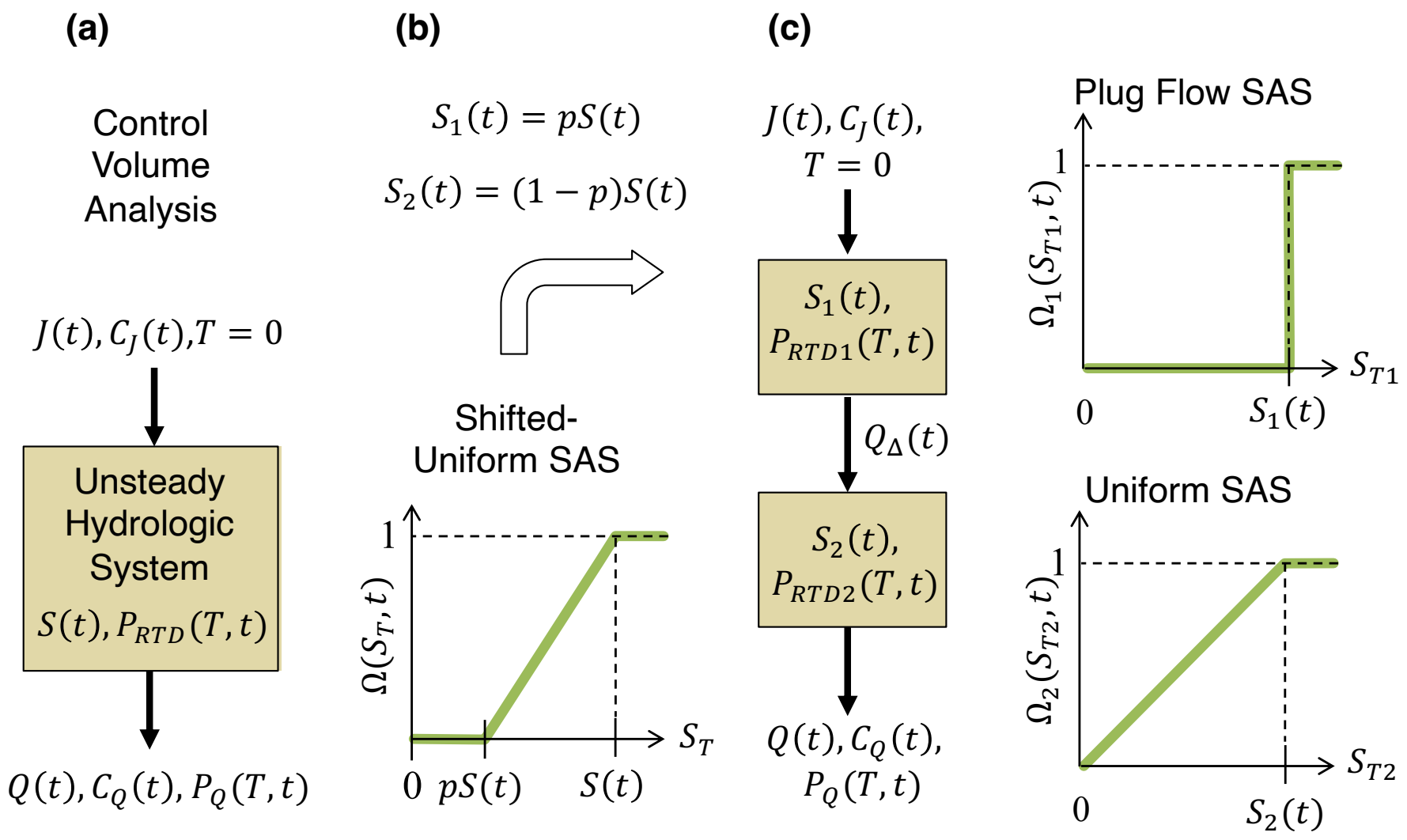
(a)
Control Volume Analysis
$J(t), C_J(t), T = 0$
Unsteady Hydrologic System
$S(t), P_{RTD}(T,t)$
$Q(t), C_Q(t), P_Q(T,t)$
(b)
$S_1(t) = pS(t)$
$S_2(t) = (1-p)S(t)$
Shifted-Uniform SAS
$\Omega(S_T, t)$
1
0
$pS(t)$
$S(t)$
S_T
(c)
$J(t), C_J(t), T = 0$
$S_1(t), P_{RTD1}(T,t)$
$Q_\Delta(t)$
$S_2(t), P_{RTD2}(T,t)$
$Q(t), C_Q(t), P_Q(T,t)$
Plug Flow SAS
$\Omega_1(S_{T1}, t)$
1
0
$S_1(t)$
S_{T1}
Uniform SAS
$\Omega_2(S_{T2}, t)$
1
0
$S_2(t)$
S_{T2}

Figure 2.

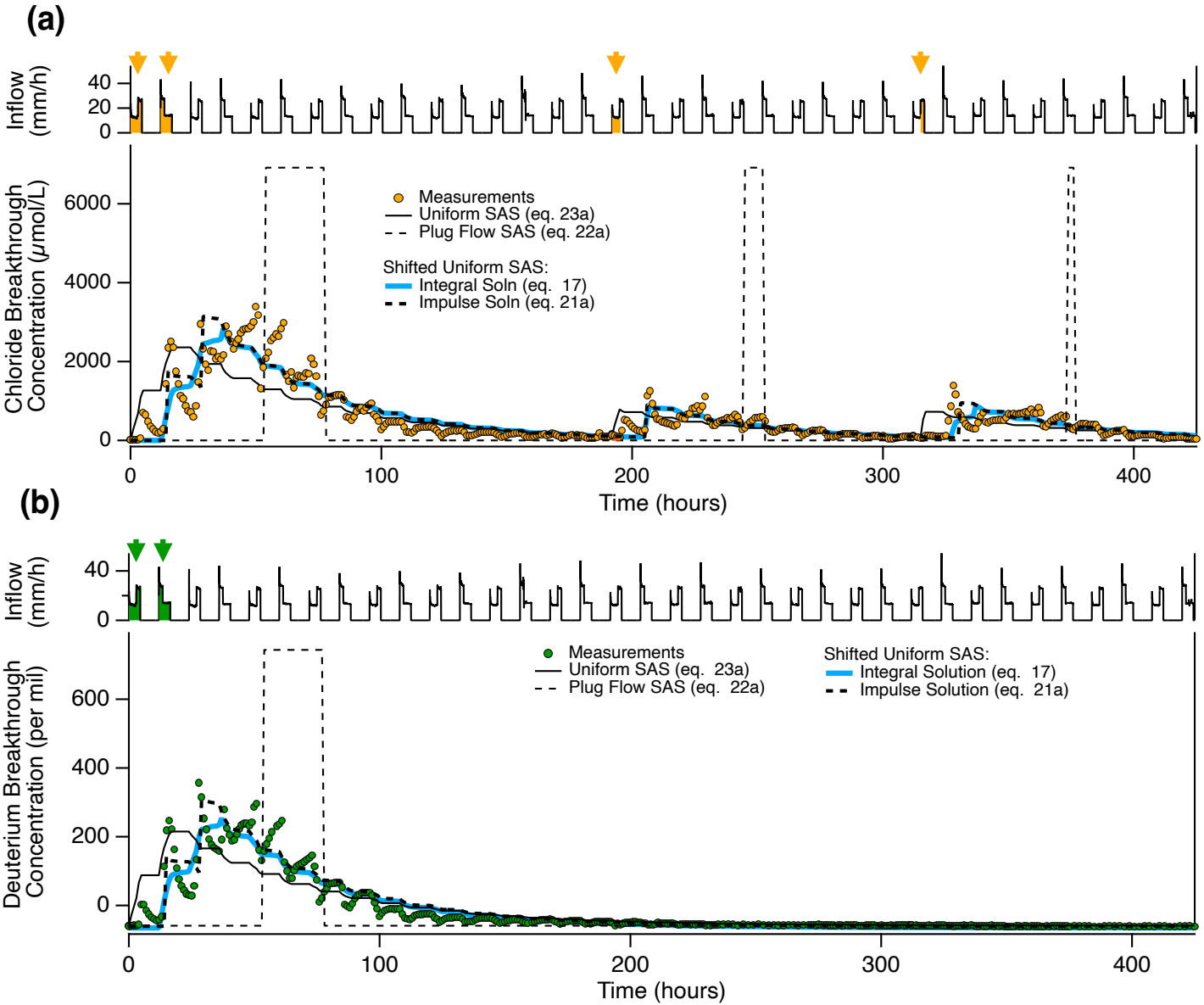
(a)
Inflow (mm/h)
40
20
0
Chloride Breakthrough Concentration (μmol/L)
6000
4000
2000
0
Measurements
Uniform SAS (eq. 23a)
Plug Flow SAS (eq. 22a)
Shifted Uniform SAS:
Integral Soln (eq. 17)
Impulse Soln (eq. 21a)
0
100
200
300
400
Time (hours)
(b)
Inflow (mm/h)
40
0
Deuterium Breakthrough Concentration (per mil)
600
400
200
0
Measurements
Uniform SAS (eq. 23a)
Plug Flow SAS (eq. 22a)
Shifted Uniform SAS:
Integral Solution (eq. 17)
Impulse Solution (eq. 21a)
0
100
200
300
400
Time (hours)

Figure 3.

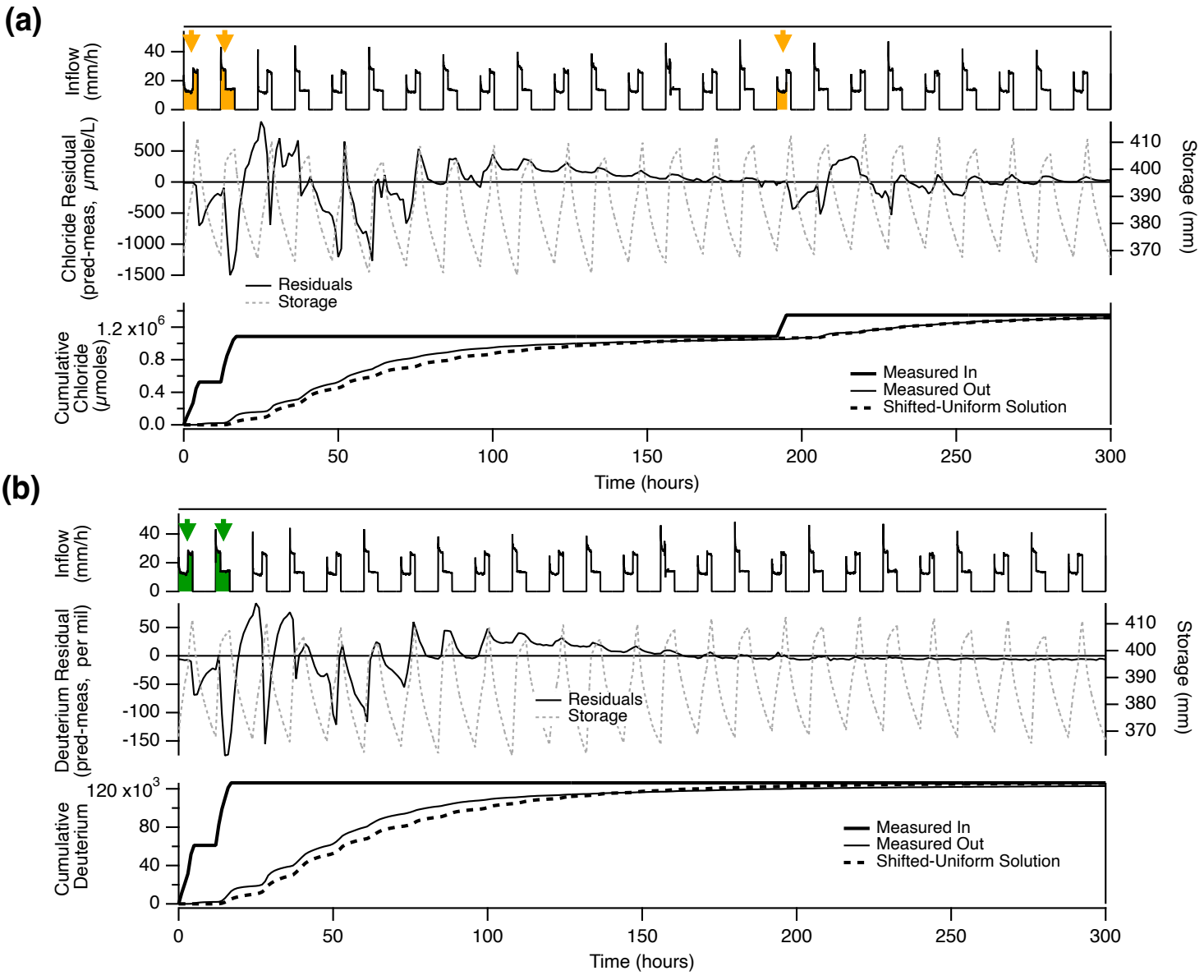
(a)
Inflow (mm/h)
40
20
0
Chloride Residual (pred-meas, μmole/L)
500
0
-500
-1000
-1500
Residuals
Storage
410
400
390
380
370
Storage (mm)
Cumulative Chloride (μmoles)
1.2 x10^6
0.8
0.4
0.0
Measured In
Measured Out
Shifted-Uniform Solution
0
50
100
150
200
250
300
Time (hours)
(b)
Inflow (mm/h)
40
20
0
Deuterium Residual (pred-meas, per mil)
50
0
-50
-100
-150
Residuals
Storage
410
400
390
380
370
Storage (mm)
Cumulative Deuterium
120 x10^3
80
40
0
Measured In
Measured Out
Shifted-Uniform Solution
0
50
100
150
200
250
300
Time (hours)

Figure 4.

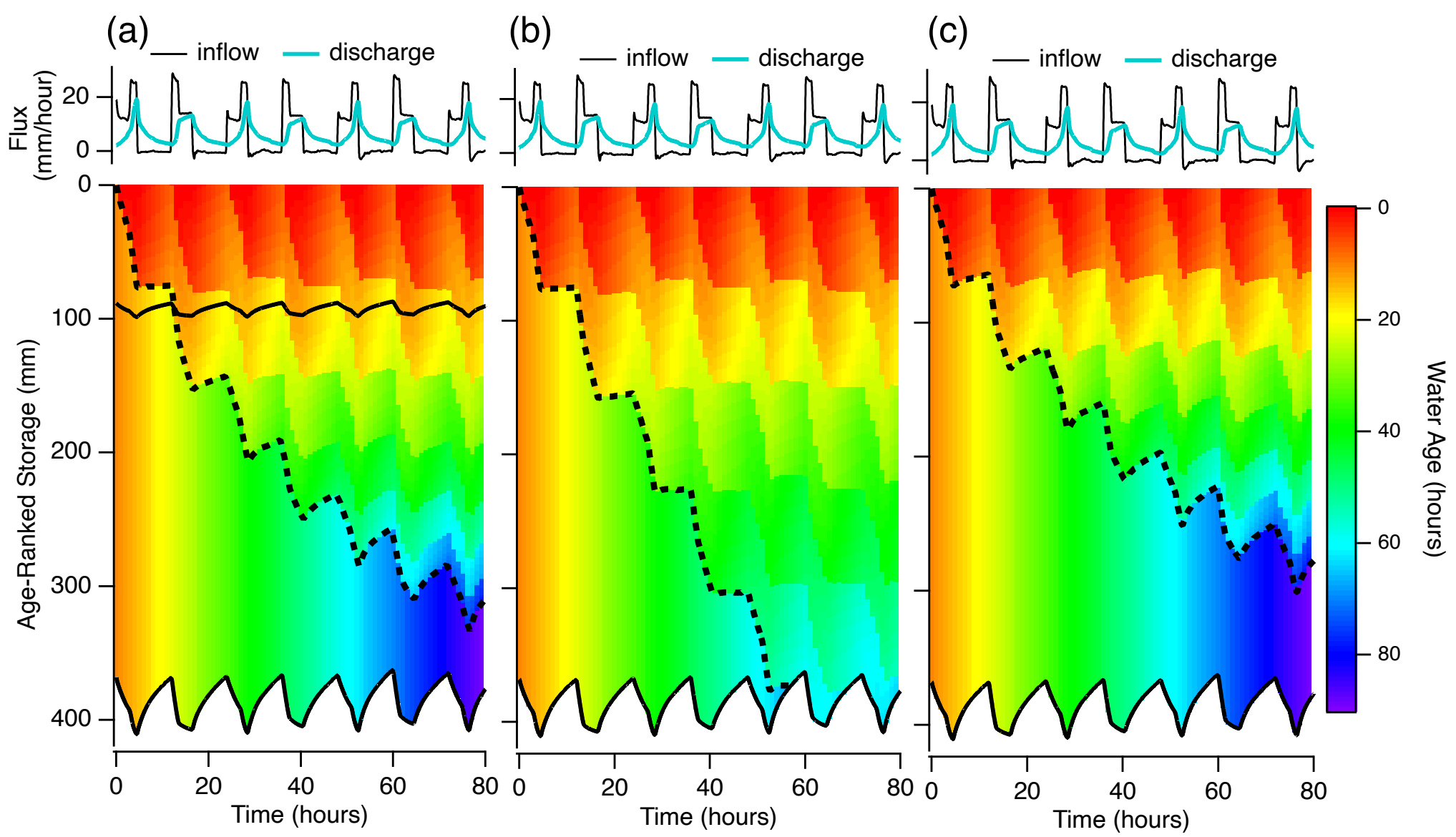
(a)
(b)
(c)
inflow
discharge
Flux (mm/hour)
20
0
Age-Ranked Storage (mm)
100
200
300
400
0
20
40
60
80
Time (hours)
Water Age (hours)

Figure 5.

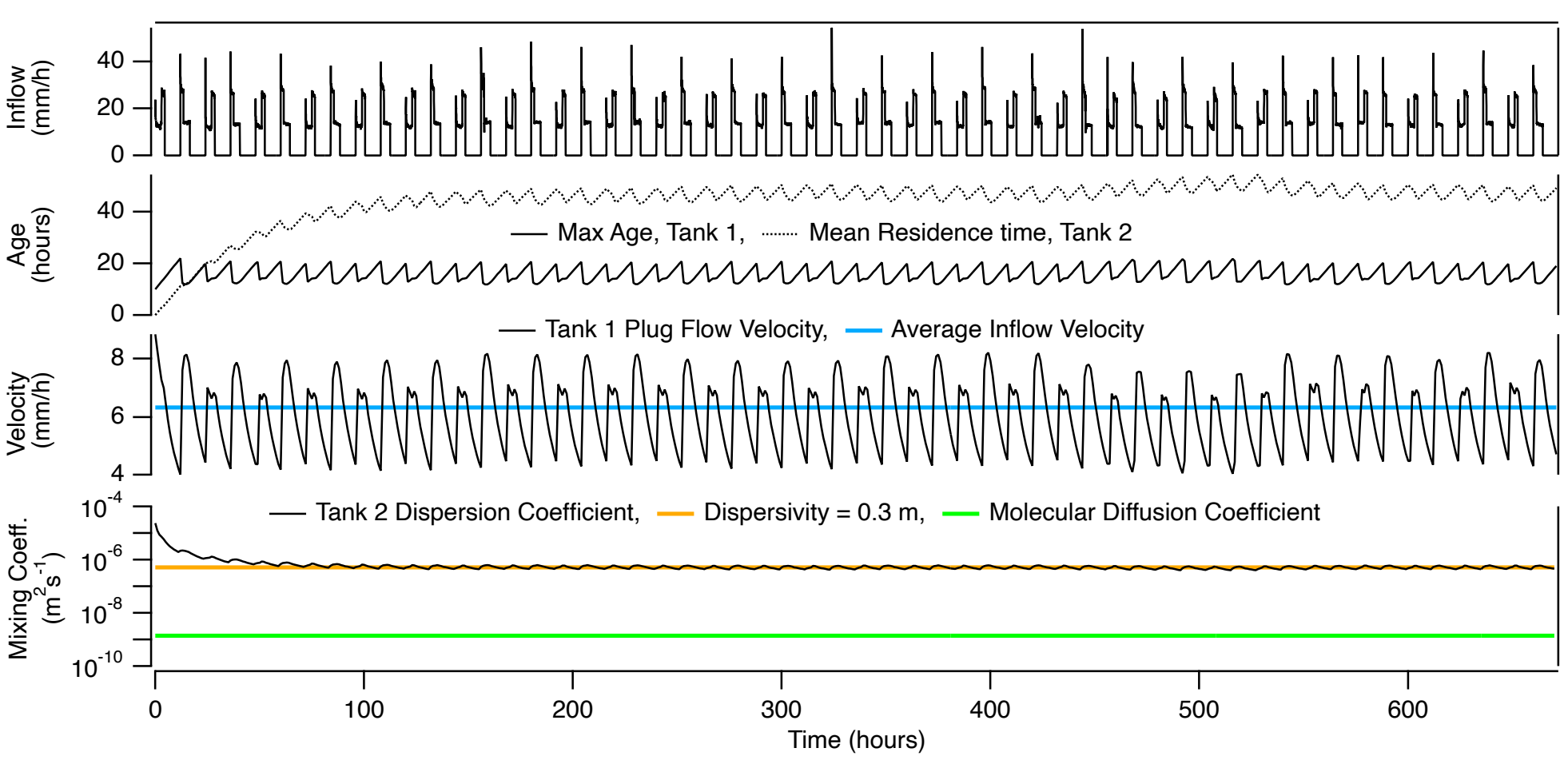
Inflow (mm/h)
40
20
0
Age (hours)
40
20
0
Max Age, Tank 1,
Mean Residence time, Tank 2
Tank 1 Plug Flow Velocity,
Average Inflow Velocity
Velocity (mm/h)
8
6
4
Mixing Coeff. (m2 s-1)
10-4
10-6
10-8
10-10
Tank 2 Dispersion Coefficient,
Dispersivity = 0.3 m,
Molecular Diffusion Coefficient
0
100
200
300
400
500
600
Time (hours)